

An Adaptive Event-based Data Converter for Always-on Biomedical Applications at the Edge

Mohammadali Sharifshazileh^{1,2}, Giacomo Indiveri^{1,2}

¹Institute of Neuroinformatics, University of Zurich and ETH Zurich;

²Zentrum für Neurowissenschaften Zürich.

Abstract—Typical bio-signal processing front-ends are designed to maximize the quality of the recorded data, to allow faithful reproduction of the signal for monitoring and off-line processing. This leads to designs that have relatively large area and power consumption figures. However, wearable devices for always-on biomedical applications do not necessarily require to reproduce highly accurate recordings of bio-signals, provided their end-to-end classification or anomaly detection performance is not compromised. Within this context, we propose an adaptive Asynchronous Delta Modulator (ADM) circuit designed to encode signals with an event-based representation optimally suited for low-power on-line spiking neural network processors. The novel aspect of this work is the adaptive thresholding feature of the ADM, which allows the circuit to modulate and minimize the rate of events produced with the amplitude and noise characteristics of the signal. We describe the circuit’s basic mode of operation, we validate it with experimental results, and characterize the new circuits that endow it with its adaptive thresholding properties.

Index Terms—Bio-signal, Asynchronous Delta Modulator, Spiking Neural Network, Neuromorphic

I. INTRODUCTION

Electrophysiological recordings are the basis for a large number of diagnostic tools in medicine [1]. Most common are recordings of cardiac function, muscle function, nerve transmission, and brain function. To achieve high reliability in off-line data analysis, or to provide medical experts with accurate bio-signal recordings, classical bio-medical devices are designed to produce very high signal quality recordings. This is directly related to the performance of signal acquisition and digitization, which is evaluated in terms of signal-to-noise ratio, linearity, resolution and sampling rate. State-of-the-art biomedical recording systems employ the most advanced integrated analog and digital signal processing methods to address those challenges using data compression, hardware sharing and time interleaving [2]–[4]. For these systems, digital filtering and heavy post processing introduce extensive power/bandwidth overhead that often leads to large area and high power consumption.

However, bio-medical applications at the edge, i.e., applications that use wearable devices for always-on monitoring and on-chip classification of bio-signals, typically do not need such high signal-to-noise ratios in their front-end processing stages. Rather than reproducing the recorded signal as faithfully as possible, the goal of these devices is to operate continuously throughout the day, and detect events of interest, such as heart beat anomalies [5], [6] or High Frequency Oscillations (HFOs),

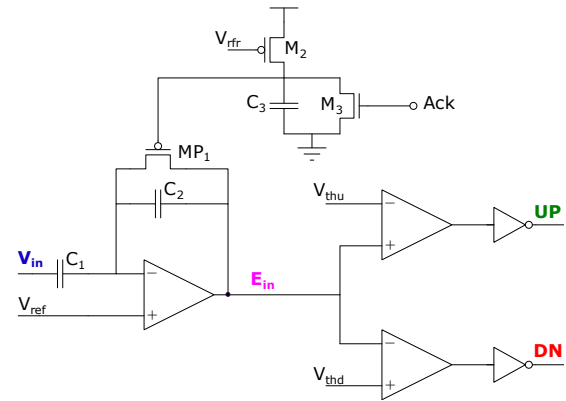


Fig. 1: ADM circuit. The analog input voltage V_{in} is converted into UP and DN pulses (spikes) for further processing by SNN circuits. The ADM spike rate depends on the comparator thresholds V_{thu} and V_{thd} .

which have been identified as relevant bio-markers of the epileptogenic zone in epilepsy patients [7], [8]. Therefore, for these use-cases, the most stringent requirements are low power and area. A promising approach to satisfy these requirements, is to employ Spiking Neural Networks (SNNs) implemented using analog/digital circuits with dynamics that are well matched to those of the signals they are designed to process [9], [10]. As these neuromorphic processors expect spikes as the input, it is important to develop bio-signal acquisition front-ends that pre-process and convert the biomedical sensory signals into streams of events. A typical front-end of this type would comprise a Low-Noise Amplifier (LNA) [11], [12], followed by one or more filtering stages, and then by an Asynchronous Delta Modulator (ADM) [13] and a low-power SNN processing module [14]–[16]. Several examples of applications that follow this approach have already been demonstrated using pre-recorded data-sets with fixed parameter settings [5], [6], [8], [13], [17]. However, in real-world applications, the amplitude of the signals being measured may change over time (e.g., if the subject sweats, changes temperature, or if the wearable device shifts and moves), and the parameters of the system may need to be adjusted at run-time. In this work we focus on the ADM block, analyzing how the circuit parameters affect the encoding of the signal, and we extend it by proposing a novel circuit that adjusts the ADM parameters continuously,

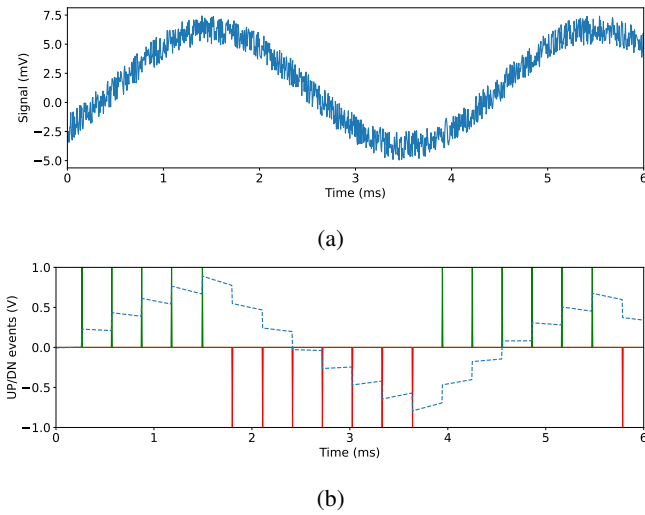


Fig. 2: Experimental results. (a) Measured response of a LNA circuit that receives in input a sine-wave attenuated to micro-Volt levels compatible with real bio-signals; (b) Response of the ADM to the waveform of (a), producing the encoded UP and DN events. The dashed line represents the signal reconstructed in software using these events (with arbitrary units).

adapting to the changes in the average background activity, while preserving the sensitivity to large changes, or anomalies in the signal. We propose analog circuits that calculate on-line the best parameters and demonstrate the adaptive ADM features on HFO signals, for which it is important to produce events only for signals with amplitudes higher than the average background, and reduce, as much as possible, the generation of events for the background activity [8].

II. THE ASYNCHRONOUS DELTA MODULATOR (ADM)

A circuit diagram of the ADM, originally proposed in [13], is shown in Fig. 1. This circuit belongs to the family of delta modulation encoders first proposed in the 1960s for communication [18] and recently adapted for event-based communication systems [19]. It consists of an input Operational Transconductance Amplifier (OTA) with a capacitive divider gain stage, two comparators, and additional inverters that produce the UP or DN digital voltages when the change in the amplified version of the input signal, (E_{in}), either increases above the reference voltage, V_{ref} , by V_{thu} or decreases below V_{ref} by V_{thd} . When either of these digital signals switch, additional logic (not shown) asserts an active-high Ack signal, which in turn resets the OTA output to V_{ref} and resets the UP and DN pulses, which are transmitted to further processing stages implemented using SNN neuromorphic processors. This reset state will be held for a “refractory period” determined by the values of the capacitor C_3 and the bias voltage V_{rfr} . The number of the UP and DN pulses depends both on the features of the input signal (amplitude and frequency) and on the ADM parameters: the comparator thresholds and the refractory period.

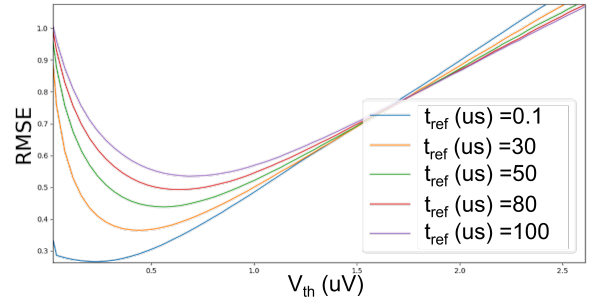


Fig. 3: Root-mean-square of the ADM spikes reconstruction error Vs. V_{th} for various values of t_{ref}

The maximum rate of pulses is hard-limited by the circuit’s refractory period. If we consider a sine-wave as the input signal, then the impact of signal related parameters and the circuit parameters on the rate of spikes generated by the ADM can be expressed as:

$$R_s \propto \frac{A \cdot f}{T_{rfr} \cdot V_{th}} \quad (1)$$

where R_s represents the ADM spike rate for a sine wave of amplitude A and frequency f ; the parameter T_{rfr} represents the refractory period, and $V_{th} := V_{thu} - V_{ref} = V_{ref} - V_{thd}$ is the comparator threshold (assuming UP and DN thresholds are equal).

Figure 2 shows experimental results measured from the ADM fabricated using a standard 180 nm Complementary Metal-Oxide-Semiconductor (CMOS) process [8]. The input signal was a sine-wave that was attenuated down to a peak-to-peak range of $100 \mu V$, off-chip and passed through an LNA with gain set to 38 dB. The resulting input sine for the ADM is depicted in Fig. 2a. For this control experiment the threshold parameters for UP and DN spikes are kept constant and symmetric. The events produced by the ADM are plotted in Fig. 2b.

Accumulative addition/subtraction of the V_{th} value at the respective UP and DN spike times would result in a reconstruction of the input from the output spikes (e.g., see dashed line in Fig. 2b). The reconstructed trace drifts away from the baseline due to the asynchronous and open-loop nature of delta-encoding, so to remove this drift effect, a high-pass filter is often applied to the staircase reconstructed signal.

The accuracy of the data conversion can be quantified by calculating the Root Mean Squared-Error (RMSE) between the original signal and the reconstructed one. Figure 3 shows the effect of the two circuit parameters (refractory period and comparator threshold) on the reconstruction and the corresponding RMSE. This analysis also shows that ADM hyperparameters, V_{th} and T_{rfr} , can be tuned to minimize the RMSE. The fact that RMSE has a non-zero minimum is due to the bounded spiking rate of the ADM, limited by the refractory period.

III. ADAPTIVE ADM

To ensure autonomous long-time operation of bio-signal processing devices in real-world embedded applications, the ADMs should include variable gain and an automatic threshold adjusting mechanisms to compensate for changes that might occur in the signal (e.g., due to electrode movement or changing conditions of the subject). To this end, we have improved the ADM in Fig.1 in two directions. First, we implemented a variable capacitor (2-bit switch, four capacitance values) in the feedback of the ADM amplifier (C_2 in Fig. 1) to add an extra degree of freedom on the gain of the front-end. This can help improving the dynamic range of bio-signal acquisition system, for capturing information in both high amplitude low-frequency signals and low-amplitude high-frequency ones. The second and more important improvement comes in the form of the adaptive threshold detection module we present in Fig. 4.

The block diagram of this circuit is depicted in Fig. 4a. It operates by tracking the envelope of the signal through a source follower integrator (Fig. 4b); the envelope is then fed into two Low Pass Filters (LPFs) implemented using current-mode Differential Pair Integrator (DPI) circuits [20] (see Fig.4c), which are then used to produce a digital voltage to enable and disable a track-and-hold, depending on the changes in amplitude of the original signal.

For sufficiently larger input signals, it has been shown that the output current of the DPI circuit can be described with the following equation [9] similar to a first-order low-pass filter:

$$\tau \frac{dI_{out}}{dt} + I_{out} = I_{in} \quad (2)$$

where $\tau = \frac{C_{U_T}}{\kappa I_T}$

The DPI1 and DPI2 filters are configured with different time constant (τ) parameters, such that their output currents I_{out1} and I_{out2} exhibit different step-response rise-times. This differentiating behavior in the presence of high-amplitude-frequency activity, alongside with properly adjusted DC component of these currents, results in output traces that cross each other when sudden changes in the envelope of the input signal occur.

To compare the traces I_{out1} and I_{out2} and detect when they cross over we used a current-mode Winner-Take-All (WTA) circuit, shown in Fig.4d [21]. When the cross-over occurs the WTA generates a pulse, which, for stability reasons, is extended using a pulse extender (PEX) circuit of the type presented in [14]. This extended pulse is used to open the switch of DPI 3 and keep the circuit in hold-mode. In this way the DPI 3 capacitor only stores the values of the envelope computed on the average background activity of the signal, and ignores the large changes in the signal. The result of this chain of operations is the setting of the ADM spiking threshold parameter, V_{th} , to a value proportional to the average background activity of the bio-signal for small fluctuations, and holding this value for periods of the signal that exhibit large fluctuations. This leads to an ADM setting that produces a large number of spikes to faithfully encode signals of interests, and zero or few spikes in response to the noisy background activity.

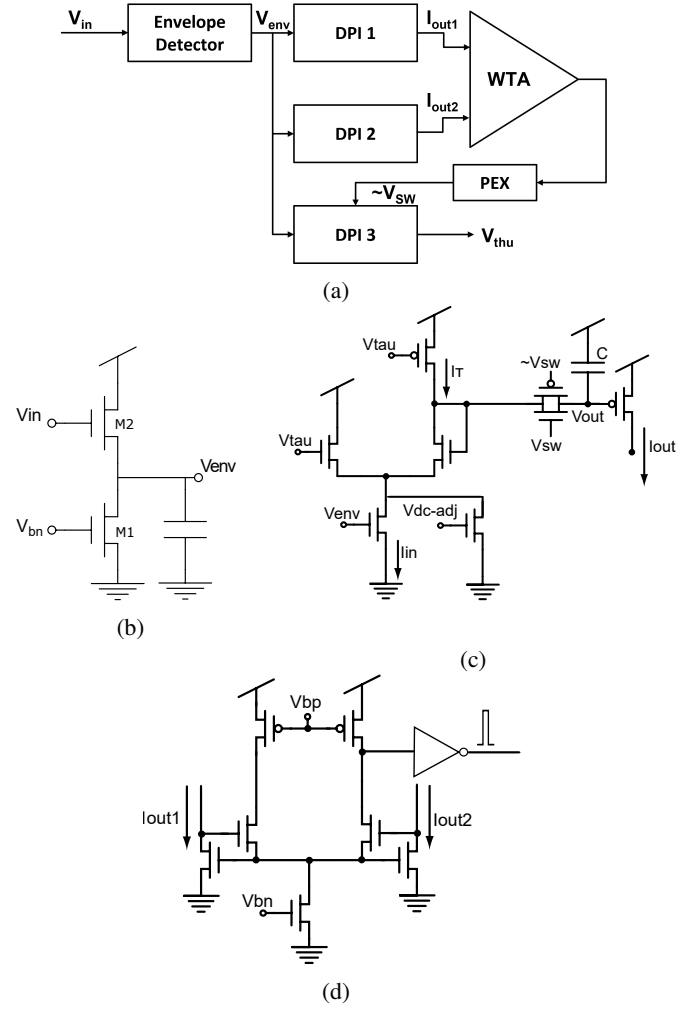


Fig. 4: Adaptive ADM threshold-detection. (a) block diagram of the non-linear adaptive scheme adopted; (b) source follower integrator used to produce the signal representing the envelope of the input; (c) DPI low-pass filter circuit with tunable cut-off frequency and controllable “hold” switch. The DPI 1 and DPI 2 blocks do not have this gating switch, while the DPI 3 block has it, controlled by the V_{sw} voltage; (d) Winner-Take-All (WTA) circuit used to compare the output currents of DPI 1 and DPI 2 and produces an active high pulse when $I_{out1} < I_{out2}$. This pulse gets extended to produce V_{sw} .

Circuit simulation results of the proposed adaptive threshold detection circuit are shown in Fig. 5. The input is a snippet of an Intracranial EEG (iEEG) signal recorded with 2 KHz sampling rate that is filtered in the 80-250 Hz frequency band [22]. This signal contains HFOs, characterized by high fluctuations from the average background activity. The envelope of this signal, extracted by the source follower, is very stable during background activity and increases in response to the high-amplitude changes (see the orange trace in the top plot of Fig. 5). The output currents of the DPIs 1 and 2 in response to the envelope signal are depicted in the second row of Fig. 5. Note that the output current of DPI 2 is always smaller than the

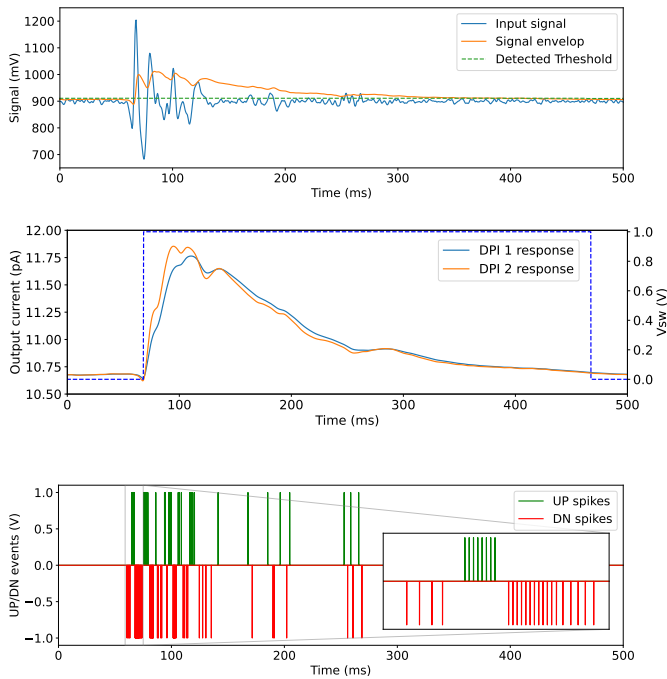


Fig. 5: Adaptive ADM simulation results. The top row shows a trace of pre-recorded iEEG, it's envelope, and the V_{th} parameter automatically detected. The middle row shows the output of the two DPI filters used to detect outlier regions which do not belong to the average background activity. The dashed represents the digital voltage that gates the updates to the V_{th} signal in these regions. The bottom row shows the UP and DN spikes generated by the ADM circuit with the V_{th} computed in this way. Note how the average background regions do not produce events. The inset in the plot shows the spikes produced for the first falling-rising-falling phases of the high-frequency oscillation.

DPI 1 output current, when the envelope is constant. However as the envelope increases rapidly, the DPI 2 filter follows it more quickly than the DPI 1 filter, and its output current crosses the DPI 1 output current. This cross-over is detected by a WTA circuit that continuously compares the two currents and produces a digital voltage pulse when the cross-over occurs. This output pulse however is typically shorter than the full length of the event (it stays high only while $I_{out2} > I_{out1}$). So to ensure a stable V_{th} , the pulse is extended to cover the full time-window of typical high-amplitude events, which depends on the nature of the bio-signal, the time-constant of the envelope detector circuit, and time-constant of the DPI 3 filter. The result is a smooth and stable spiking threshold produced by the DPI 3 circuit (see dashed green line in the top row of Fig. 5). The bottom row of Fig. 5 shows how the output spikes generated by the ADM only encode the relevant events and ignore the background activity, thanks to the adaptive thresholding module.

IV. DISCUSSION

The major bottleneck holding back analog front-ends from being used with SNN devices in low-power bio-signal processing edge applications is the data conversion block. Optimizing the performance of conventional data converters is often performed by changing the design towards minimizing quantization error. Indeed, knowing the characteristics of the input signal, one could optimize the hyperparameters of the ADM to minimize the reconstruction error as shown in Fig.3. However, as the goal of the SNN processing pipeline is to classify or recognize features of interest in the input, rather than reconstructing the original signal faithfully, it is important to optimize resource usage (including area and power budget of the front-end) considering the end-to-end performance of the full system. Mixed-signal SNNs heavily rely on analog front-ends that provide input spikes that encode frequency- and amplitude-specific information present in analog input signal. While most clinically relevant bio-signals tend to have sparse high-amplitude events, some such as Local Field Potentials (LFPs) are slow and gradual. So adding flexibility and adaptability to the analog front-ends is of critical importance.

V. CONCLUSIONS

In this article, we discussed about the benefits of using ADM circuits in bio-signal acquisition front-ends. We demonstrated with experimental data their characteristics, and proposed a set of circuits for improving their performance, by endowing them with non-linear filtering properties that would allow them to change their parameters on-line, adapting to changes in their operating conditions or changes in the input signals. We provided circuit simulation results, and validated them using clinically relevant bio-signals that contain long traces of average background activity, for which it is desirable to produce sparse spiking activity, if any, and short high frequency and high amplitude pulses, for which it is important to have ADM parameters that can encode the signal with high accuracy. Future developments will include integrating these circuits on a new design and testing them on Electroencephalography (EEG), Electrocardiogram (ECG), and electromyography (EMG) signals.

REFERENCES

- [1] L. Peeples, "Core concept: The rise of bioelectric medicine sparks interest among researchers, patients, and industry," *Proceedings of the National Academy of Sciences*, vol. 116, no. 49, pp. 24 379–24 382, 2019. [Online]. Available: <https://www.pnas.org/content/116/49/24379>
- [2] M. Chae, W. Liu, Z. Yang, T. Chen, J. Kim, M. Sivaprakasam, and M. Yuce, "A 128-channel 6mw wireless neural recording ic with on-the-fly spike sorting and uwb transmitter," in *Solid-State Circuits Conference Digest of Technical Papers (ISSCC), 2008 IEEE International*, Feb. 2008, pp. 143–603.
- [3] H. Hosseiniejad, A. Jannesari, and A. Sodagar, "Data compression in brain-machine/computer interfaces based on the walsh-hadamard transform," *IEEE transactions on biomedical circuits and systems*, vol. 8, no. 1, pp. 129–137, 2014.
- [4] A. Sodagar, K. Wise, and K. Najafi, "A fully integrated mixed-signal neural processor for implantable multichannel cortical recording," *IEEE Transactions on Biomedical Engineering*, vol. 54, no. 6, pp. 1075–1088, 2007.
- [5] F. Bauer, D. Muir, and G. Indiveri, "Real-time ultra-low power ECG anomaly detection using an event-driven neuromorphic processor," *Biomedical Circuits and Systems, IEEE Transactions on*, vol. 13, no. 6, pp. 1575–1582, Dec. 2019.
- [6] F. Corradi, S. Pande, J. Stuijt, N. Qiao, S. Schaafsma, G. Indiveri, and F. Cathoor, "ECG-based heartbeat classification in neuromorphic hardware," in *International Joint Conference on Neural Networks (IJCNN)*. IEEE, 2019, pp. 1–8.
- [7] T. Fedele, S. Burnos, E. Boran, N. Krayenbühl, P. Hilfiker, T. Grunwald, and J. Sarnthein, "High frequency oscillations detected in the intracranial EEG of epilepsy patients during interictal sleep, patients' electrode location and outcome of epilepsy surgery," *Collaborative Research in Computational Neuroscience*, 2017.
- [8] M. Sharifshazileh, K. Burelo, J. Sarnthein, and G. Indiveri, "An electronic neuromorphic system for real-time detection of high frequency oscillations (HFOs) in intracranial EEG," *Nature Communications*, vol. 12, no. 1, pp. 1–14, 2021.
- [9] E. Chicca, F. Stefanini, C. Bartolozzi, and G. Indiveri, "Neuromorphic electronic circuits for building autonomous cognitive systems," *Proceedings of the IEEE*, vol. 102, no. 9, pp. 1367–1388, Sep. 2014.
- [10] G. Indiveri and Y. Sandamirskaya, "The importance of space and time for signal processing in neuromorphic agents," *IEEE Signal Processing Magazine*, vol. 36, no. 6, pp. 16–28, 2019.
- [11] G. Atzeni, J. Guichemerre, A. Novello, and T. Jang, "A 1.01 NEF low-noise amplifier using complementary parametric amplification," *IEEE Transactions on Circuits and Systems I: Regular Papers*, vol. 69, no. 3, pp. 1065–1076, 2022.
- [12] L. Liu, D. Gao, Y. Tian, Y. Yu, and Z. Qin, "A low mismatch and high input impedance multi-channel time-division multiplexing analog front end for bio-sensors," *IEEE Sensors Journal*, vol. 22, no. 7, pp. 6755–6763, 2022.
- [13] F. Corradi and G. Indiveri, "A neuromorphic event-based neural recording system for smart brain-machine-interfaces," *Biomedical Circuits and Systems, IEEE Transactions on*, vol. 9, no. 5, pp. 699–709, 2015.
- [14] S. Moradi, N. Qiao, F. Stefanini, and G. Indiveri, "A scalable multicore architecture with heterogeneous memory structures for dynamic neuromorphic asynchronous processors (DYNAPs)," *Biomedical Circuits and Systems, IEEE Transactions on*, vol. 12, no. 1, pp. 106–122, Feb. 2018.
- [15] C. Frenkel and G. Indiveri, "ReckOn: A 28 nm sub-mm² task-agnostic spiking recurrent neural network processor enabling on-chip learning over second-long timescales," in *2022 IEEE International Solid-State Circuits Conference Digest of Technical Papers (ISSCC)*. IEEE, 2022, pp. 468–470.
- [16] C. Frenkel, M. Lefebvre, J.-D. Legat, and D. Bol, "A 0.086-mm² 12.7-pj/SOP 64k-synapse 256-neuron online-learning digital spiking neuromorphic processor in 28-nm CMOS," *IEEE Transactions on Biomedical Circuits and Systems*, vol. 13, no. 1, pp. 145–158, 2019.
- [17] Y. Ma, B. Chen, P. Ren, N. Zheng, G. Indiveri, and E. Donati, "EMG-based gestures classification using a mixed-signal neuromorphic processing system," *IEEE Journal on Emerging and Selected Topics in Circuits and Systems*, vol. 10, no. 4, pp. 578–587, 2020.
- [18] R. Steele, *Delta modulation systems*. Pentech Press & Halsted Press, 1975.
- [19] M. Yang, S.-C. Liu, and T. Delbruck, "Comparison of spike encoding schemes in asynchronous vision sensors: Modeling and design," in *IEEE International Symposium on Circuits and Systems (ISCAS)*. IEEE, 2014, pp. 2632–2635.
- [20] C. Bartolozzi, S. Mitra, and G. Indiveri, "An ultra low power current-mode filter for neuromorphic systems and biomedical signal processing," in *Biomedical Circuits and Systems Conference, (BioCAS), 2006*. IEEE, 2006, pp. 130–133.
- [21] J. Lazzaro, S. Ryckebusch, M. Mahowald, and C. Mead, "Winner-take-all networks of $o(n)$ complexity," in *Advances in neural information processing systems (NIPS)*, D. Touretzky, Ed., vol. 2. San Mateo - CA: Morgan Kaufmann, 1989, pp. 703–711.
- [22] T. Fedele, S. Burnos, E. Boran, N. Krayenbühl, P. Hilfiker, T. Grunwald, and J. Sarnthein, "Resection of high frequency oscillations predicts seizure outcome in the individual patient," *Scientific Reports*, vol. 7, p. 13836, Oct. 2017.